



Boron adsorption onto activated carbon and amorphous carbon prepared from sucrose dehydration

Mouna Jaouadi*, Ahmed Hichem Hamzaoui

Useful Materials Valorization Laboratory, National Centre of Research in Materials Science, Technologic Park of Borj Cedria, B.P. 73, 8027 Soliman, Tunisia, Tel. +216 99 434 202; email: ing.mouna@gmail.com (M. Jaouadi)

Received 9 January 2018; Accepted 28 January 2019

ABSTRACT

The comparison of performances of two materials based on carbon, industrial activated carbon and carbon obtained from sucrose dehydration, for boron removal from aqueous solution was achieved. For that, both materials were at first characterized by the determination of N_2 adsorption–desorption measurements, X-ray diffraction, infrared and Raman spectroscopies, thermal analysis (TGA-DTA), “Boehm” titration and pH of the point zero charge. The tests of adsorption show that despite its lowest specific surface area, amorphous carbon from sucrose dehydration exhibits the highest boron adsorption uptake (1.8 mg g^{-1}) compared with the industrial activated carbon. The surface chemistry particularly rich in carboxylic groups for the prepared carbon was responsible for the high boron adsorption. Based on the results of this study Langmuir is the best isotherm model describing adsorption of boron onto carbon-based materials, as it gave the maximum R^2 value.

Keywords: Sucrose; Dehydration; Amorphous carbon; Adsorption; Boron

1. Introduction

In nature, boron occurs in the form of undissociated orthoboric acid, partially dissociated borate anions in the form of polyborates, complexes of transition metals and fluoroborate complexes [1]. In water, boron appears predominantly in the form of boric acid.

Boron and its compounds must be removed from drinking water with high concentrations. The boron concentration recommended by the World Health Organization for drinking water is 2.4 mg L^{-1} .

The amount of boron in water depends on many factors such as the geochemical nature of the drainage area and input from industrial effluents.

Boron is an important nutrient for plants, the range between deficient and toxic levels is very narrow. Some species such as blackberry and citrus are highly susceptible to boron with a tolerance level less than $0.5 \text{ mg L}^{-1} B$ [2]. As

well known, boron will be able to damage the reproducibility of living organisms at sufficiently high concentrations.

The removal of boron from aqueous solution requires several technologies. However, some methods face serious limitation in boron removal due to the aqueous chemistry of boron-containing species such as in case of reverse osmosis [3]. Reverse osmosis could effectively remove boron but is costly and requires adjusting pH to the high level [4,5].

Some inorganic materials were used for boron removal from water through precipitation [6], complexation, and adsorption [7].

The boron adsorption sites for carbon based-materials are mainly the hydroxyl groups present at the surface. Carbon-based materials have got considerable attention during the past decades. Numerous types of structures of carbon have been prepared.

Carbon exists in a variety of stable forms such as graphite, diamond, nanotubes, and amorphous carbon.

Activated carbon is well known as a material used in both gas and liquid phases. The large surface area of activated

* Corresponding author.

carbon enables it to adsorb diverse pollutants one among which is boron. Using activated carbon as an adsorbent, better performance could be achieved with the impregnation of activated carbon with chemical compounds. Celik et al. [8] have studied the adsorption of boron using salicylic acid as an impregnant and the result showed the significant enhancement with 15% removal for pure activated carbon and up to 25% for modified activated carbon.

Amorphous carbon has a lot of interests due to its unique properties such as high hardness, low friction coefficient, and chemical inertness. Optical and electrical properties of amorphous carbon can be tuned by manipulating the sp^2 and sp^3 bonding ratio [9].

In addition to that, amorphous carbon is known by the high biocompatibility and the high hemocompatibility properties [10]. Recently there are many researchers that confirm that amorphous carbon provides accessible complexation sites for boron species [11].

In this work, amorphous carbon was produced from sucrose dehydration. Industrial activated carbon and amorphous carbon are used as adsorbents to remove boron from aqueous solution. The structure and surface properties of these adsorbents were characterized using Fourier transform infrared spectroscopy (FTIR), Raman spectroscopy, powder X-ray diffraction (XRD), "Boehm" titrations, measurements of pH of the point zero charge (pH_{PZC}), thermal analysis (TGA-DTA) and N_2 adsorption-desorption at 77 K.

2. Materials and methods

2.1. Preparation of amorphous carbon

Amorphous carbon was obtained from the dehydration of sucrose. Sucrose is commonly known as table sugar, and it is obtained from sugar cane or sugar beets. It is a non-reducing disaccharide composed of glucose and fructose linked via their anomeric carbons.

In this work, 50 g of sucrose was mixed with 50 mL of concentrated sulfuric acid in a tall-form beaker. The color of the mixture changes from white to yellow and to black. At this point, the mixture will begin to expand out of the beaker.

Industrial activated carbon, which is used as an adsorbent to remove boron from aqueous solution, was provided by Sigma-Aldrich (France).

2.2. Characterization of the adsorbents

2.2.1. Determination of the acidic surface functional groups

Boehm titrations quantify the basic and oxygenated acidic surface groups on activated carbons [12,13]. Surface functional groups such as carboxyl (RACOOH) and P-containing acidic groups, lactones (RAOCO), phenols (Ar-OH), carbonyls or quinones (RR'C,O) and basic groups were determined.

Surface functional groups were quantified by assuming that NaOH did not react with the RR'C,O groups; Na_2CO_3 did not react with RR'C,O and RAOH groups, and that $NaHCO_3$ only reacted with RACOOH groups and the P-containing acidic groups.

Experimentally, about 0.1 g of each sample (activated carbon, amorphous carbon) was mixed in a closed polyethylene flask with 20 mL of 0.02 mol L⁻¹ aqueous reactant solution (NaOH, or Na_2CO_3 , or $NaHCO_3$). The mixtures were stirred for 48 h at a constant speed of 150 rpm at room temperature before being filtered through 0.45 mL membrane filters (Millipore 405314). To determine the oxygenated group's content, back-titrations of the filtrate (10 mL) were performed with standardized HCl (0.02 mol L⁻¹). The numbers of all acidic sites were calculated under the assumption that NaOH neutralizes carboxylic, phenolic and lactonic groups. Basic groups contents were also determined by back titration of the filtrate with NaOH (0.02 mol L⁻¹) after agitation of the activated carbon (0.1 g) in HCl (0.02 mol L⁻¹) for 48 h.

2.2.2. pH of point zero charge

The point of zero charge (pH_{PZC}) describes the condition when the electrical charge density on a surface is null. The pH_{PZC} was determined by the so-called pH drift method [12]. The pH of a deoxygenized suspension of the activated carbon (0.15 g) in an NaCl aqueous solution (50 mL at 0.01 mol L⁻¹) was adjusted to successive initial values between 2 and 10. The suspensions were stirred for 48 h under N_2 and the final pHs were measured and plotted against the initial pHs. The pH_{PZC} was determined at the value for which $pH_{final} = pH_{initial}$.

2.2.3. FTIR spectroscopy

The FTIR spectra were recorded with an EQUINOX 55 FTIR spectrophotometer (Bruker, Germany) on dried pellets obtained by pressing a mixture of 1 mg of each sample (well dried) and 300 mg of dried spectrometric grade KBr under 350 MPa. Spectra were recorded in the 4,000–400 cm⁻¹ range with a 4 cm⁻¹ resolution; 64 scans were performed on each sample.

2.2.4. Raman characterization

Raman analyses were carried out at room temperature using a Dilor XY-800 confocal micro-Raman spectrometer coupled with a microscope. The spectra were recorded in backscattering geometry, at 514.5 nm radiation beam from an Ar-Kr laser-focused on the sample (spot of 2 μ m power of 20 mW). Baseline corrected spectra were computed using Origin 6.0.

2.2.5. X-ray diffraction

The XRD diagrams were obtained on a Philips X'Pert PRO MRD (PW 3050, Germany) diffractometer at the $CuK_{\alpha 1}$ radiation (1.54056 Å). The measurements were recorded under Bragg-Brentano geometry in the 5°–70° 2 θ range (0.05 step).

2.2.6. Thermal analysis

Thermogravimetric analyses (TGA-DTA) were carried out using a SETARAM apparatus. Initial sample masses of 17.5 mg

were placed in a hemispherical crucible. The use of small masses was necessary to reduce the effects of side reactions as well as mass and heat transfer limitations. Experiments were performed under argon at heating rate of $5^{\circ}\text{C min}^{-1}$.

2.2.7. N_2 adsorption–desorption at 77 K

N_2 adsorption–desorption isotherms of the activated carbons were measured at 77 K using an automatic sorptometer (ASAP 2020, Micromeritics, USA), after degassing activated carbon and amorphous carbon samples overnight at 250°C . The specific surface areas of the activated carbons were calculated using the Brunauer–Emmett–Teller (BET) equation, assuming 0.162 nm^2 area for the nitrogen molecule. As negative unrealistic C factors were obtained by applying the BET model in the relative pressure range from 0.05 to 0.3, the BET specific surface areas were then preferentially computed in the relative pressure range from 0.01 to 0.05, as for the microporous materials.

2.3. Boron adsorption isotherms

Equilibrium adsorption was studied at 22°C for 3 h using 1 g of sample in 100 mL of solution containing boron concentrations in the $5\text{--}100 \text{ mg L}^{-1}$ range. The initial pH was set to the pKa value of $\text{H}_3\text{BO}_3/\text{B}(\text{OH})_4^-$, that is, 9.26, by addition of a 0.1 mol L^{-1} NaOH solution.

After adsorption, the dispersions were centrifuged at 180 rpm for 15 min, and the boron concentrations of the recovered solutions were determined by spectrophotometry (PerkinElmer (France), Lambda 22, quartz cells) at 410 nm using azomethine-H as a complexant. The adsorption uptake of boron (q_e) onto each adsorbent (AC, amorphous carbon) was calculated from the mass balance relationship [11]:

$$q_e = \frac{(C_i - C_e)V}{W} \quad (1)$$

where V (mL) is the solution volume, C_i and C_e (mg L^{-1}) are concentrations of the initial and final solutions of boron, respectively; and w (g) is the dried adsorbent mass.

3. Results and discussion

3.1. Boehm titrations and pH_{PZC}

Table 1 shows that the pH_{PZC} of amorphous carbon is around 4.49. Such value indicates that, at pH below approximately 4.49, the surface groups of the adsorbent will be protonated, that is, positively charged. At $\text{pH} = 4.49$, the net charge of the surface of the adsorbents will be equal to zero. Finally, at pH values above 4.49, the surface groups will be deprotonated and the surface will exhibit negative charge.

The pH_{PZC} value of industrial activated carbon is in agreement with the one (i.e., 9) measured by Gamze et al. [14].

Table 1 also shows the highest amount of acidic groups was formed in amorphous carbon obtained from sucrose dehydration. The high value in acidic groups could be explained by the reaction with sulfuric acid and the possible

Table 1

pH_{PZC} and total surface acid groups of the adsorbents (determined by Boehm titrations)

	Activated carbon	Amorphous carbon
Carboxylic (mmol g^{-1})	0.2	2.65
Lactonic (mmol g^{-1})	0.2	2.41
Phenolic (mmol g^{-1})	0.04	0.27
Acidic (mmol g^{-1})	0.44	5.33
pH_{PZC}	9	4.49

formation of sulfonic acid groups. In amorphous carbon, among the various oxygenated groups, the carboxylic groups were found at the highest content (2.65 mmol g^{-1}). The low pH_{PZC} value of amorphous carbon is in agreement with the predominance of surface acid groups (5.33 mmol g^{-1}).

3.2. FTIR spectroscopy

FTIR spectra of activated carbon and amorphous carbon are shown in Fig. 1. For all the samples, the stretching vibrations of the $-\text{OH}$ groups observed around 3400 cm^{-1} were partly attributed to the residual presence of adsorbed water in the carbons.

For all the carbon materials, the band at 1700 cm^{-1} is assigned to the $-\text{C}=\text{O}$ bond in carbonyl, carboxyl, anhydride and lactone. The intensity of this band was found to be weak in activated carbon but quite strong in amorphous carbon confirming the dehydration of sucrose in the presence of concentrated sulfuric acid.

The presence of the bending vibrations (out of plane) of C–H bonds ranging from 900 to 700 cm^{-1} both in amorphous carbon spectrum might be the signature of the dehydration of sucrose.

The band around 1220 cm^{-1} is typically attributed to the C–O band.

The band intensity around 2920 cm^{-1} was characteristic of C–H stretching of aliphatic moieties; most likely associated with the glycidic part of sucrose [15]. Particularly, this band was more intense for amorphous carbon.

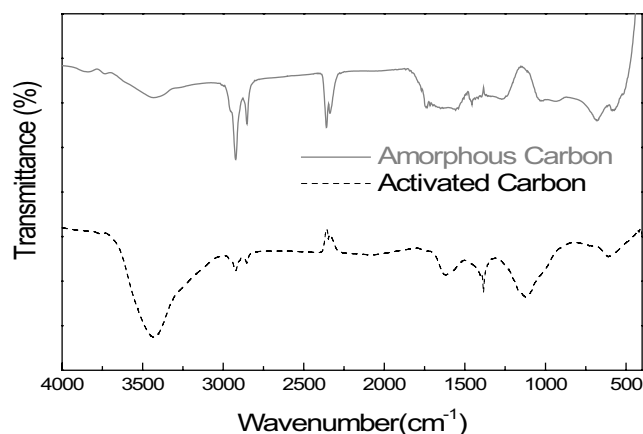


Fig. 1. FTIR spectra of activated carbon and amorphous carbon.

The band at $1,250\text{ cm}^{-1}$ reflects the presence of sulfur in amorphous carbon, it might be due to the presence of sulfonic acid groups. Moreover, the bands in the $700\text{--}900\text{ cm}^{-1}$ region might refer to S–O–R stretching [11].

It will be concluded that valuable information about the chemical compositions of the carbon based-materials were provided by FTIR spectra.

3.3. Raman spectroscopy

Raman spectroscopy is a non-destructive tool for structural characterization of carbon films.

The Raman spectra of activated carbon and amorphous carbon (Fig. 2) exhibit two broad Raman bands at about $\sim 1,360$ and $\sim 1,570\text{ cm}^{-1}$ assigned to the disordered structure mode (*D* mode) and the graphitic structure mode (*G* mode), respectively [16].

The I_D/I_G ratio (where I_D and I_G are the intensities of *D* and *G* bands, respectively) can be related to the coherence length along the basal plane (L_a).

The I_D/I_G ratios are 0.76 for amorphous carbon and 1.5 for activated carbon, which reveals that the disorder degree of amorphous carbon surfaces increases after the dehydration of sucrose.

Intensity ratio I_D/I_G and *G*-band position have been reported to depend on the sp^2 content in the material [17]. In amorphous carbons, I_D/I_G is a measure of the size of the sp^2 phase organized in rings. If I_D/I_G is negligible, then the sp^2 phase is mainly organized in chains, or even if rings are present, the Π bonds are not fully delocalized on the rings [17].

It should be noted that Raman spectroscopy is a suitable tool for the characterization of carbon-based materials. The I_D/I_G ratio has been successfully used to evaluate the degree of disorder in amorphous carbon obtained from sucrose dehydration.

3.4. X-ray diffraction

The XRD results are presented in Fig. 3. Two broad maxima, in activated carbon diffractogram, corresponding to (002) and (101) reflections of a turbostratic carbon structure

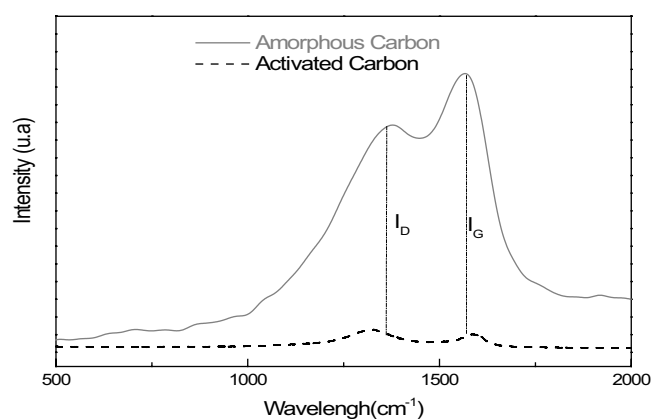


Fig. 2. Raman spectra of amorphous carbon and activated carbon.

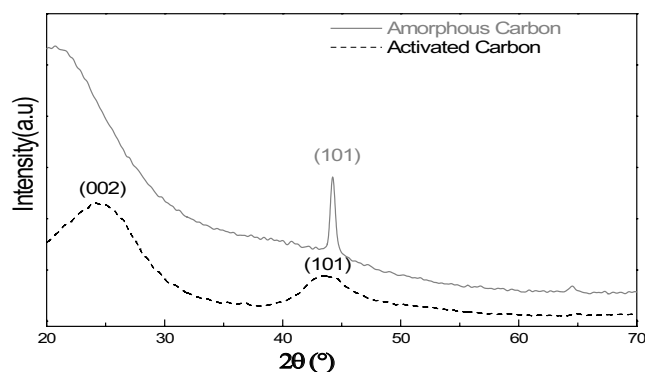


Fig. 3. X-ray diffraction of amorphous carbon and activated carbon.

[18]. The peak at around 25.4° ($d = 0.348\text{ nm}$) was due to the stacking structure of aromatic layers of carbon [19].

The spectrum of pure amorphous carbon showed a peak at $2\theta \sim 43.5^\circ$ that corresponds to the (1 0 1) band and a broad peak in the range of $20^\circ\text{--}45^\circ$ (2θ), which was typical for amorphous solids, confirmed the absence of an ordered crystalline structure, this result is in good agreement with the literature [20].

XRD analysis is a fundamental method for studying the amorphous carbon obtained by dehydration of sucrose.

3.5. Porosity characterization

Fig. 4 shows the N_2 adsorption–desorption isotherms (at 77 K) of activated carbon and amorphous carbon.

Activated carbon exhibits isotherms with evident hysteresis loops in the relative pressure range of about 0.4–0.9.

The surface properties of the carbon materials are summarized in Table 2. The amorphous carbon showed very low specific surface area ($1.73\text{ m}^2\text{ g}^{-1}$).

The carbon from sucrose dehydration, with a small specific surface area, was mainly mesoporous contrary to activated carbon.

It may be concluded that the sucrose dehydration leads to a sample showing a well-developed porous texture so it

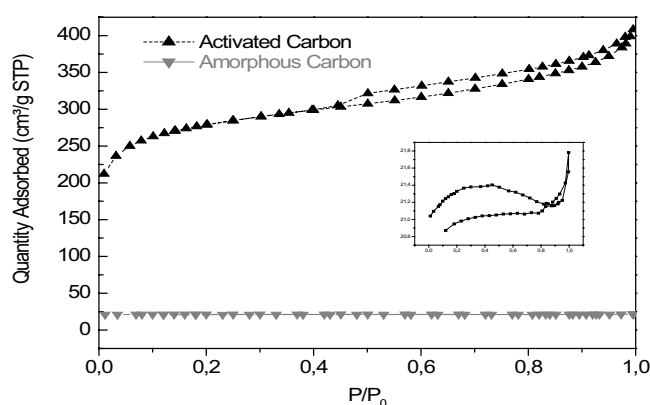


Fig. 4. N_2 adsorption–desorption isotherms at 77 K of amorphous carbon and activated carbon.

Table 2
Porosity characteristics of activated carbon and amorphous carbon

	Activated carbon	Amorphous carbon
S_{BET} ($\text{m}^2 \text{g}^{-1}$)	957.26	1.73
Diameter (\AA)	53.35	86.43
Micropore volume ($\text{cm}^3 \text{g}^{-1}$)	0.27	–
Micropore area ($\text{cm}^3 \text{g}^{-1}$)	601.36	–
Mesopore area ($\text{cm}^3 \text{g}^{-1}$)	355.9	–
External area ($\text{cm}^3 \text{g}^{-1}$)	355.89	2.50
V_{tot} ($\text{cm}^3 \text{g}^{-1}$)	0.59	0.000902

is possible to prepare amorphous carbon showing tailored properties in terms of micro- or mesoporous texture and surface area.

3.6. TGA-DTA

In order to investigate the thermal stability of carbon adsorbents, we carried out TGA-DTA experiments. This technique is quite useful as it provides information about the temperature range where these adsorbents are stable. The results of thermal analysis of TGA are shown in Fig. 5(a). For both carbon materials, the first mass loss steps, from about 22°C to 150°C, concerns mainly the loss of physically adsorbed water.

The TGA curves reveal more accurate differences in the thermal behavior of the samples. The amorphous carbon exhibits the highest total mass loss (about 50% at 1,000°C) compared with activated carbon. For amorphous carbon, TGA signal shows a more important weight loss in the range 300°C–500°C than activated carbon. This was attributed to the decomposition of the amorphous carbon.

The decomposition of amorphous carbon at a lower temperature can be explained by the characteristics of the organic compounds present in sucrose before the dehydration with sulfuric acid. The results of thermal analysis of DTA are shown in Fig. 5(b).

The strong endothermic peak at 111°C confirms the gradual removal of the H_2O molecules in both carbon materials. The second endothermic peak at 450°C of amorphous carbon is assigned to the degradation of carbon material. It can occur from 100°C to 400°C for carboxylic acid groups, from 200°C to 600°C for lactone groups, and over 600°C for phenol, carbonyl, ether, quinone, and anhydride groups which includes CO [21].

The endothermic reaction occurred on the DTA curve of amorphous carbon at about 760°C, which should be attributed to the elimination of carbon dioxide and sulfur dioxide, which was released from the dehydration of sucrose with sulfuric acid.

3.7. Boron adsorption

As shown in Fig. 6, the boron adsorption isotherms at 25°C can be divided into two stages in the range of experimental equilibrium concentrations. Boron removal

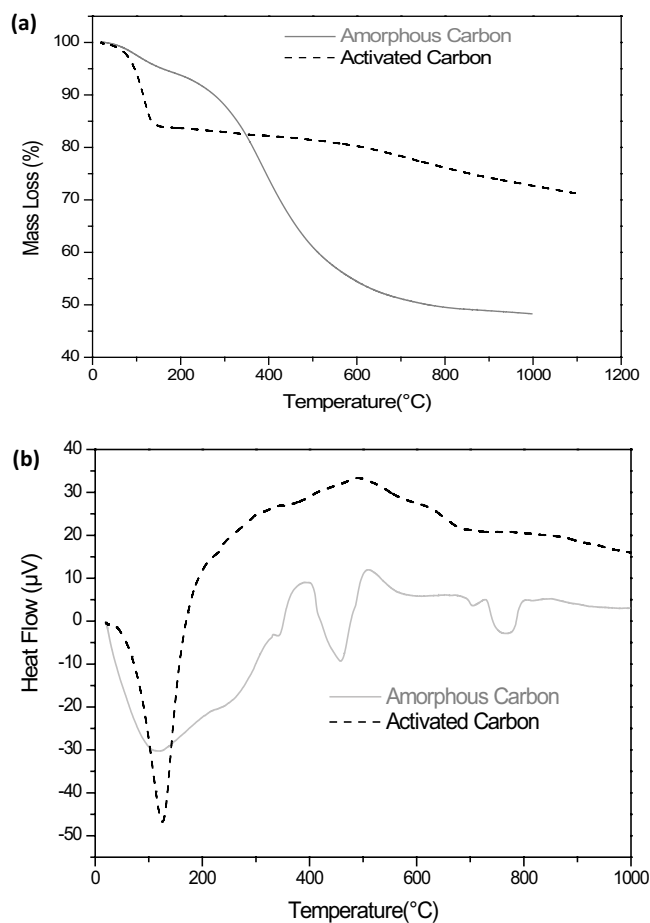


Fig. 5. Thermogravimetry (TGA) (a) and differential thermal analysis (DTA) and (b) of activated carbon and amorphous carbon.

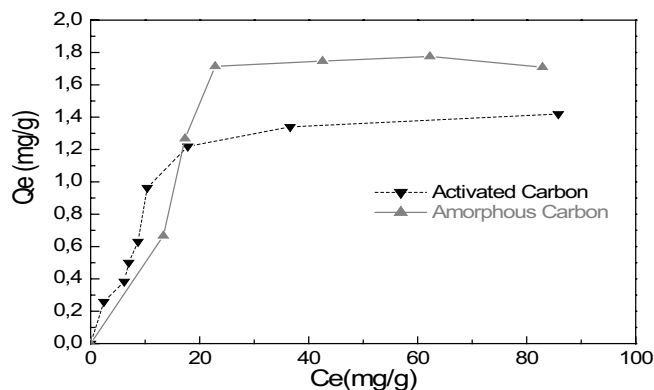


Fig. 6. Experimental adsorption isotherms of boron on amorphous carbon and activated carbon ($m = 1 \text{ g}$, $V = 100 \text{ mL}$, $T = 25^\circ\text{C}$, $\text{pH} = 9.26$, contact time = 3 h).

capabilities measured at pH 9.26 in water, the highest one was found for the adsorption on the amorphous carbon (1.8 mg g^{-1}) compared with activated carbon (1.3 mg g^{-1}). At the working pH (~ 9.26), the main existing forms of boron were both H_3BO_3 and $\text{B}(\text{OH})_4^-$ [22]. As the pH of point zero charge of activated carbon and amorphous carbon were

found to be acidic, their surfaces at the working pH were negatively charged. Thus the main adsorbed species were H_3BO_3 and $B(OH)_4^-$ underwent repulsion from the carbon surfaces [23].

Fig. 6 shows the high affinity of boron for the amorphous carbon surface. The highest capacity for amorphous carbon despite its lowest specific surface area was explained by the presence of high content of carboxylic groups formed through the dehydration of sucrose. This result confirmed that adsorption of boron on carbon materials is mainly governed by the complexation of boron species with electron donors (mainly OH groups or carbonyl groups).

The amorphous carbon sample exhibits a remarkably high capability of boron removal ($\sim 1.8 \text{ mg g}^{-1}$ at a concentration of 20 ppm) higher than the value of 1.41 mg g^{-1} reported by Mouna et al. [11].

The relationship between the amount of boron adsorbed and equilibrium concentration of boron in solution can be described by isotherms. Langmuir and Freundlich models are often used to describe the experimental isotherm data [24,25].

The Langmuir isotherm can be applied for type I equilibrium adsorption [26]:

$$q_e = q_0 \left(\frac{b \times C_e}{1 + b C_e} \right) \quad (2)$$

where C_e is the equilibrium concentration of the boron solution (mg L^{-1}) and q_e is the amount adsorbed at equilibrium (mg g^{-1}), q_0 (mg g^{-1}) and b (L mg^{-1}) are Langmuir constants related to the adsorption capacity and the energy of adsorption.

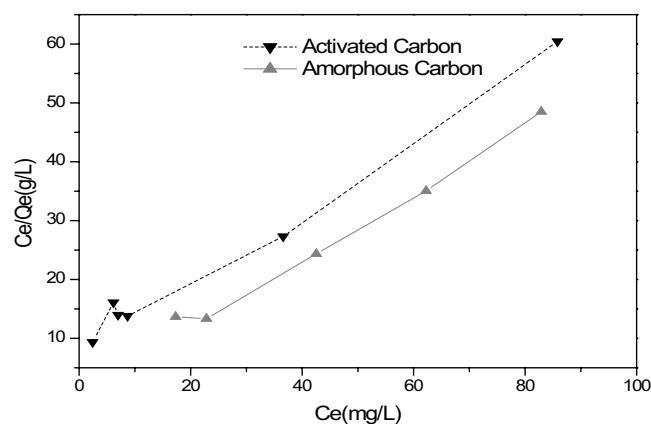


Fig. 7. Langmuir plots for boron removal by adsorption (at pH 9.26 and 22°C).

The linear plot of C_e/q_e vs. C_e shows that adsorption follows a Langmuir isotherm (Fig. 7), the constants q_0 and b were calculated from the slope and intercept of the linear plots and are presented in Table 3. As shown in Table 3, the correlation coefficients found of the isotherms by the Langmuir-model are higher than 0.99. The increased b value can be used to explain that the mechanism of adsorption is different for amorphous carbon and activated carbon and the affinity was enhanced after dehydration of sucrose.

The Freundlich model would be applicable. The Freundlich equation is represented by the equation:

$$\log q_e = \log K + \frac{1}{n} \log C_e \quad (3)$$

where K (mg g^{-1}) is the Freundlich capacity constant and n is the Freundlich intensity constant. A plot of linear Freundlich equation $\log C_e$ vs. $\log q_e$ is shown in Fig. 8.

The fit of data to the Freundlich equation may indicate the heterogeneity of the activated carbon surface. The low value of K showed difficulty uptake of boron from aqueous solution with a low adsorptive capacity of the sorbent [27]. The n values are related to the Giles classification, S , L , and C type isotherm. $n > 1$ correspond to S shape, $n = 1$ to C type, and $n < 1$ to L type [28]. As can be seen from Table 3, the n value of the boron sorption isotherms on activated carbon confirms S -shape. The Freundlich constant n should have a value lying in the range of 1–10 for the classification of adsorption as favorable.

Boron adsorption onto industrial activated carbon fits both the Freundlich and the Langmuir isotherms [29], but at

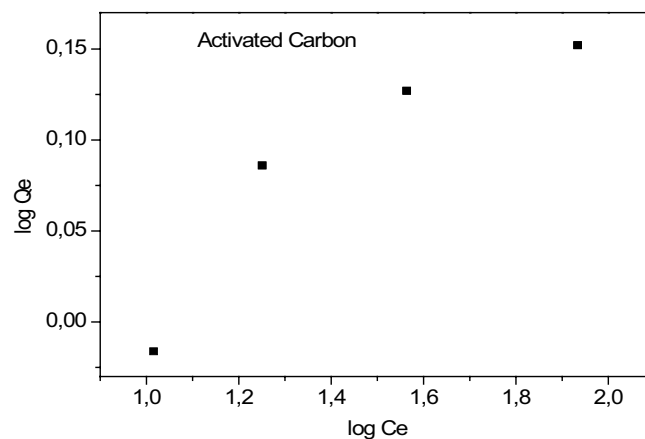


Fig. 8. Freundlich plots for boron removal by adsorption onto activated carbon (at pH 9.26 and 22°C).

Table 3
Langmuir and Freundlich constants

	Langmuir			Freundlich		
	q_0 (mg g^{-1})	b (L mg^{-1})	R^2	n	K (mg g^{-1})	R^2
Activated carbon	1.3	0.06	0.993	5.88	$10 \exp(-0.15)$	0.92
Amorphous carbon	1.85	0.25	0.994	–	–	–

low boron concentration, adsorption fits neither Freundlich nor the Langmuir isotherms [30]. Based on all results, it can be concluded that the amorphous carbon prepared from sucrose dehydration allowed a high capacity for boron removal from an aqueous solution. This opens new perspectives in the field of adsorbent materials, in order to prepare very efficient carbon adsorbents for boron remediation by the dehydration of carbohydrates.

4. Conclusion

In this work, an amorphous carbon was prepared from sucrose dehydration. The amorphous character of the atomic structure was confirmed by Raman spectroscopy and X-ray diffraction. Amorphous carbon displays very low specific surface areas compared with the industrial activated carbon. The surface of amorphous carbon is very rich in carboxylic groups, were an advantage for boron removal from water.

For boron removal capabilities measured at pH 9.26, the highest one was found for the adsorption on the amorphous carbon (1.8 mg g^{-1}) compared with industrial activated carbon (1.3 mg g^{-1}). The presence of very high content of carboxylic groups in the amorphous carbon prepared from sucrose dehydration allowed a high capacity for boron removal. This result confirmed that adsorption of boron on carbon-based materials is mainly governed by the complexation of boron species with electron donors (mainly OH groups).

Based on the results of this study, Langmuir is the best isotherm model describing adsorption of boron onto carbon-based materials, as it gave the maximum R^2 value.

References

- [1] A.J. Wyness, R.H. Parkaman, C. Neal, A summary of boron surface water quality data throughout the European Union, *Sci. Total Environ.*, 314 (2003) 255–269.
- [2] L. Butterwick, N. de Oude, K. Raymond, Safety assessment of boron in aquatic and terrestrial environments, *Ecotoxicol. Environ. Saf.*, 17 (1989) 339–371.
- [3] J. Wolska, M. Bryjak, Methods for boron removal from aqueous solutions—a review, *Desalination*, 310 (2013) 18–24.
- [4] D. Piotr, T. Marian, C. Jerzy, T. Jolanta, K. Joanna, Boron removal from landfill leachate by means of nanofiltration and reverse osmosis, *Desalination*, 185 (2005) 131–137.
- [5] E.H. Ezechi, M. Hasnain, R.R.B.M. Kutty, Boron in Produced water: challenges and improvements: a comprehensive review, *J. Appl. Sci.*, 12 (2012) 402–415.
- [6] P. Remy, H. Muhr, E. Plasari, I. Ouerdiane, Removal of boron from wastewater by precipitation of a sparingly soluble salt, *Environ. Prog.*, 24 (2004) 105–110.
- [7] W.W. Choi, K.Y. Chen, Evaluation of boron removal by adsorption on solids, *J. Am. Chem. Soc.*, 13 (1979) 189–196.
- [8] Z.C. Celik, B.Z. Can, M.M. Kocakerimb, Boron removal from aqueous solutions by activated carbon impregnated with salicylic acid, *J. Hazard. Mater.*, 152 (2008) 415–422.
- [9] J. Robertson, Diamond-like amorphous carbon, *Mater. Sci. Eng., R*, 37 (2002) 129–281.
- [10] R. Hauert, A review of modified DLC coatings for biological applications, *Diamond Relat. Mater.*, 12 (2003) 583–589.
- [11] J. Mouna, H. Souhaira, G. Hanen, R. Laurence, A. Noureddine, D. Laurent, Preparation and characterization of carbons from β -cyclodextrin dehydration and from olive pomace activation and their application for boron adsorption, *J. Saudi Chem. Soc.*, 21 (2017) 822–829.
- [12] S. Goldberg, Inconsistency in the triple layer model description of ionic strength dependent boron adsorption, *J. Colloid Interface Sci.*, 285 (2005) 509–517.
- [13] M.V. Lopez-Ramon, F. Stoeckli, C. Moreno-Castilla, F. Carrasco-Marin, On the characterization of acidic and basic surface sites on carbons by various techniques, *Carbon*, 37 (1999) 1215–1221.
- [14] E. Gamze, K. Yasemin, G.A. Onur, K. Tanju, Adsorption of organic contaminants by graphene nanosheets, carbon nanotubes and granular activated carbons under natural organic matter preloading conditions, *Sci. Total Environ.*, 565 (2016) 811–817.
- [15] A. Ros, M.A. Lillo-Ródenas, E. Fuente, M.A. Montes-Morán, M.J. Martín, A. Linares-Solano, High surface area materials prepared from sewage sludge-based precursors, *Chemosphere*, 65 (2006) 132–140.
- [16] R.J. Nemanich, S.A. Solin, First- and second-order Raman scattering from finite-size crystals of graphite, *Phys. Rev. B: Condens. Matter*, 20 (1979) 392–401.
- [17] A.C. Ferrari, J. Robertson, Interpretation of Raman spectra of disordered and amorphous carbon, *Phys. Rev. B: Condens. Matter*, 61 (2000) 14095–14107.
- [18] G.M. Jenkins, K. Kawamura, *Polymeric Carbons—Carbons Fibre, Glass and Char*, Cambridge University Press, Cambridge, 1976.
- [19] B. Sakintuna, Y. Yürüm, Preparation and characterization of mesoporous carbons using a Turkish natural zeolitic template/furfuryl alcohol system, *Microporous Mesoporous Mater.*, 93 (2006) 304–312.
- [20] S. Mopoung, Surface image of charcoal and activated charcoal from banana peel, *J. Microsc. Soc. Thai*, 22 (2008) 15–19.
- [21] J.L. Figueiredo, M.F.R. Pereira, M.M.A. Freitas, J.J.M. Órfão, Modification of the surface chemistry of activated carbons, *Carbon*, 37 (1999) 1379–1389.
- [22] A. Farhat, F. Ahmad, H. Arafat, Analytical techniques for boron quantification supporting desalination process: a review, *Desalination*, 310 (2013) 9–17.
- [23] Y.T. Wei, Y.M. Zheng, J.P. Chen, Design and fabrication of an innovative and environmental friendly adsorbent for boron removal, *Water Res.*, 45 (2011) 2297–2305.
- [24] D. Kavak, Removal of boron from aqueous solutions by batch adsorption on calcined alunite using experimental design, *J. Hazard. Mater.*, 163 (2009) 308–314.
- [25] N. Öztürk, D. Kavak, Boron removal from aqueous solutions by batch adsorption onto cerium oxide using full factorial design, *Desalination*, 223 (2008) 106–112.
- [26] C. Namasivayam, D. Kavitha, Removal of Congo Red from water by adsorption onto activated carbon prepared from coir pith, an agricultural solid waste, *Dyes Pigm.*, 54 (2002) 47–58.
- [27] W.J. Weber, *Physicochemical Processes for Water Quality Control*, Wiley, New York, 1972, 640 p.
- [28] M.M. Socias-Viciana, M.C. Hermosin, J. Cornejo, Removing prometryne from water by clays and organic clays, *Chemosphere*, 37 (1998) 289–300.
- [29] S. Yüksel, Y. Yürüm, Removal of boron from aqueous solutions by adsorption using fly ash, zeolite, and demineralized lignite, *Sep. Sci. Technol.*, 45 (2010) 105–115.
- [30] Y. Fujita, T. Hata, M. Nakamura, T. Iyo, T. Yoshino, T. Shimamura, A study of boron adsorption onto activated sludge, *Bioresour. Technol.*, 96 (2005) 1350–1356.